Effect of Exponential Stress Resultant on Buckling Response of Functionally Graded Rectangular Plates

K. Khorshidi[*], A. Fallah

Mechanical Engineering Department, Faculty of Engineering, Arak University, Arak, Iran.

Article info

Abstract

The effect of exponential stress resultant on buckling response of functionally graded rectangular plates based on exponential shear deformation theory is investigated in this paper. In exponential shear deformation theory, exponential functions are used in terms of thickness coordinate to include the effect of the transverse shear deformation and rotary inertia. The material properties of the functionally graded plate are assumed to vary according to a power low form according to the thickness direction. The equations of motions are derived based on Hamiltons principle. To validate the formulations, present results in specific cases are compared with available results in literature and good agreement could be seen. Finally, the influence of different parameters like power law indexes, aspect ratio, and the thickness ratio on the non-dimensional critical buckling load of rectangular FG plates are presented and discussed in detail.

Nomenclature

a	Length of the plate	b	Width of the plate
h	Thickness of the plate	ϑ	Poisson's ratio
E	Young's modulus	G	Shear modulus
ρ	Mass density	g	Power law index
u	Displacement in the x_1 direction	v	Displacement in the x_2 direction
w	Displacement in the x_3 direction	ε_{ii}	Normal strains
γ_{ij}	Shear strains	σ_{ij}	Normal stresses
τ_{ij}	Shear stresses	δ	Variation operator
U	Strain energy of the plate	W	Work done by external forces
N_2	In plane loads perpendicular to the edges $x_2 = 0, b$	N_1	In plane load perpendicular to the edges $x_1 = 0, a$
T	Kinetic energy of the plate	λ_{mn}	Natural frequency of the plate
$[K]$	Stiffness matrix	$[K_g]$	Stiffness matrix related to the in-plane forces
N_{cr}	Critical buckling load		

1. Introduction

Functionally graded materials (FGMs) are composite materials intentionally designed so that they possess desirable properties for specific applications, especially for aircrafts, space vehicles and other engineering structures under high-temperature environments. FGMs are heterogeneous composite materials in which the material properties vary continuously from one interface to the other. Those are achieved by gradually varying volume fraction of constituent materials.

The advantage of using these materials is that they can survive the high thermal gradient environment, while maintaining their structural integrity. FGMs were initially designed as thermal barrier materials for aerospace structural applications and fusion reactors. Now they are developed for the general use as structural components in high-temperature environments. Typically, a FGM is made of a ceramic and a metal for the purpose of thermal protection against large temperature gradients. The ceramic material provides the high-temperature resistance due to its low thermal conductivity while the ductile metal constituent prevents fracture due to its greater toughness. Reissner [1] developed a stress based FSDT which incorporates the effect of shear and Mindlin [2] employed displacement based approach. In Mindlin's theory, transverse shear stress is assumed to be constant through the thickness of the plate, but this assumption violates the shear stress free surface conditions on the top and bottom surfaces of the plate. Mindlins theory satisfies constitutive relations for transverse shear stresses and shear strains by using shear correction factor. Mokhtar et al. [3] studied buckling response of S-FGM plates in thermal environment according to first order shear deformation theory. In their study material properties varied smoothly according to thickness direction based on Sigmond distribution. Şimşek and Reddy [4] investigated buckling of functionally graded material plates based on Higher order shear deformation plate theory. Matsunaga [5] studied the vibration and buckling response of functionally graded plates by taking into account the influence of transverse shear, normal deformations, and rotatory inertia. By using the method of power series expansion of displacement components, a set of functionally graded (FG) plates was derived using Hamiltons principle. Yahia et al. [6] analyzed the wave propagation in functionally graded plates according to higher order shear deformation plate theory. Malekzadeh and Alibeygi [7] studied the free vibration of functionally graded arbitrary straight-sided quadrilateral plates under the thermal environment and based on the first-order shear deformation plate theory. The differential quadrature method was adopted to discretize the equilibrium equations. Ungbhakorn and Wattanasakulpong [8] presented thermo-elastic vibration response of functionally graded plates caring distributed patch mass-based on third order shear deformation theory. The solutions were obtained using the energy method. Furthermore, the forced vibration analysis with external dynamic load acting on the subdomain of the patch mass was discussed. Reddy [9] investigated buckling analysis of simply supported functionally graded plates based on higher order shear deformation theory (HSDT). Sayyad and Ghugal [10] presented the bending and free vibration of thick isotropic rectangular plates by using Exponential shear deformation theory. In their work a displacement based

on Exponential shear deformation theory (ESDT) was used for the bending and free vibration analysis of thick isotropic square and rectangular plates containing effect of transverse shear deformation and rotary inertia. The displacement field of the theory contains three variables like in the first order shear deformation plate theory. Khorshidi [11] studied a theory to calculate the natural frequencies of rectangular plate partially contacting bounded fluid in the bottom and vertical direction using the Rayleigh-Ritz method. In their developed model, the von Karman linear strain displacement relationships were used in order to obtain the kinetic and strain energies of the plate. Senthilnathan et al. [12] used Reddy theory to present a simplified higher order theory in which a further reduction of the functional degree of freedom was introduced by splitting up the transverse displacement in to bending and shear contributions. Khorshidi and Khodadadi [13] investigated closed-form solution for out-of-plane vibration of rectangular plates via trigonometric shear deformation theory. Khorshidi and Pagoli [14] studied analytical solution for sound radiation of vibrating circular plates coupled with piezoelectric layers. Thai and Choi [15] presented size-dependent functionally graded material for Kirchhoff and Mindlin plate models, geometric nonlinearity, and material variation through the thickness of the plate. The equations of motion were derived from Hamiltons principle based on the modified Couple stress theory, Von Karman nonlinear strains, and Power Law variation of materials through the thickness. Analytical solutions for the static bending, buckling, and free vibration problems were presented for a plate with all simply supported boundary conditions to accentuate the effects of material length scale parameter on the deflection, buckling load, and frequency. Khorshidi and Farhadi [16] performed hydrostatic vibration analysis of a laminated composite rectangular plate partially contacting with a bounded fluid. In their research, natural frequencies of the plate coupled with sloshing fluid modes were calculated using Rayleigh-Ritz method based on minimizing the Rayleigh quotient.

In the present research, buckling response of functionally graded plate according to exponential shear deformation theory is investigated. In the exponential shear deformation theory exponential functions are used in the thickness direction to include the influence of transverse shear deformation and rotary inertia. It is supposed that the material properties are changing through the thickness direction according to the power law distribution. The results of present work can be used as benchmarks for future studies.

2. Equations and Mathematics

Consider a flat rectangular FG-plate of length a, width b, and total thickness h and mixture of functionally

graded materials through the thickness as shown in Fig. 1. The plate is under in-plane loads perpendicular to the edges $x_1 = 0$, a and $x_2 = 0$, b. The properties of the plate were assumed to vary through the thickness of the plate according to a power-law distribution of the volume fractions of two materials between the two surfaces. In fact, the top surface ($x_3 = h/2$) of the plate was ceramic-rich whereas the bottom surface ($x_3 = -h/2$) was metal-rich.
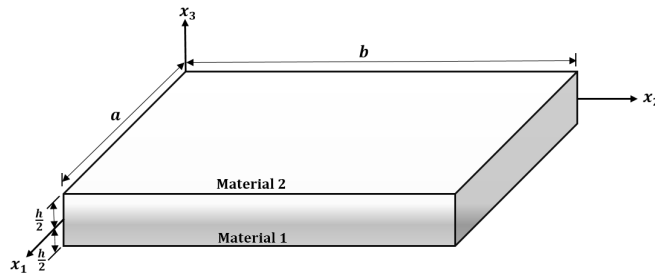

Fig. 1. Geometry of an FGM plate.

Poisson's ratio ϑ was assumed to be constant and was taken as 0.3 throughout the analysis. Young's modulus and mass density were assumed to vary continuously through the plate thickness as [9];

$$E(x_3) = (E_c - E_m)V(x_3) + E_m \qquad (1)$$

$$\rho(x_3) = (\rho_c - \rho_m)V(x_3) + \rho_m \qquad (2)$$

$$V(x_3) = \left(\frac{x_3}{h} + \frac{1}{2}\right)^g \qquad (3)$$

where g is power law index and takes only positive values. According to Eqs. (1) and (2) when the power law index g approaches zero or infinity, the plate is isotropic composed of fully ceramic or metal respectively. Typical values for metal and ceramics used in the FG plate are listed in Table 1.

Table 1
The material properties of concrete specimens.

Material	Properties		
	E(Gpa)	ϑ	ρ(kg/m^3)
Aluminum (Al)	70	0.3	2702
Alumina (Al$_2$O$_3$)	380	0.3	3800

2.1. Displacement Relations

The displacement field of the exponential shear deformation theory is given as below [13];

$$u(x_1, x_2, x_3, t) = \qquad (4a)$$

$$u_0(x_1, x_2, x_3, t) - x_3\frac{\partial w(x_1, x_2, t)}{\partial x_1} + f(x_3)\varphi_1(x_1, x_2, t)$$

$$v(x_1, x_2, x_3, t) = \qquad (4b)$$

$$v_0(x_1, x_2, x_3, t) - x_3\frac{\partial w(x_1, x_2, t)}{\partial x_2} + f(x_3)\varphi_2(x_1, x_2, t)$$

$$w(x_1, x_2, x_3, t) = w(x_1, x_2, t) \qquad (4c)$$

where $f(x_3) = x_3 e^{-2(\frac{x_3}{h})^2}$ and u, v, and w are displacements in the x_1, x_2, and x_3 directions respectively, and u_0 and v_0 are the mid-plane displacements. With the linear assumption of Von-Karman strain, the displacement strain field will be as follows:

$$\varepsilon_{11} = \frac{\partial u}{\partial x_1} = \frac{\partial u_0}{\partial x_1} - x_3\frac{\partial^2 w}{\partial x_1^2} + f(x_3)\frac{\partial \varphi_1}{\partial x_1} \qquad (5a)$$

$$\varepsilon_{22} = \frac{\partial u}{\partial x_2} = \frac{\partial u_0}{\partial x_2} - x_3\frac{\partial^2 w}{\partial x_2^2} + f(x_3)\frac{\partial \varphi_2}{\partial x_2} \qquad (5b)$$

$$\gamma_{12} = \frac{\partial u}{\partial x_2} + \frac{\partial v}{\partial x_1} = \frac{\partial u_0}{\partial x_2} + \frac{\partial v_0}{\partial x_1} - 2x_3\frac{\partial^2 w}{\partial x_1 \partial x_2}$$

$$+ f(x_3)\left(\frac{\partial \varphi_1}{\partial x_2} + \frac{\partial \varphi_2}{\partial x_1}\right) \qquad (5c)$$

$$\gamma_{13} = \frac{\partial u}{\partial x_3} + \frac{\partial w}{\partial x_1} = \frac{df(x_3)}{dx_3}\varphi_1 \qquad (5d)$$

$$\gamma_{23} = \frac{\partial v}{\partial x_3} + \frac{\partial w}{\partial x_2} = \frac{df(x_3)}{dx_3}\varphi_2 \qquad (5e)$$

In the Eq. (5), ε_{ii} are normal strains and γ_{ij} are shear strains. Considering Hooke's Law for stress field, the normal stress σ_{33} was assumed to be negligible in comparison with plane stresses σ_{11} and σ_{22}. Thus, stress-strain relationships will be as follows:

$$\sigma_{11} = \frac{E(x_3)}{1-\vartheta^2}(\varepsilon_{11} + \vartheta\varepsilon_{22}) = \frac{E(x_3)}{1-\vartheta^2}\left[f(x_3)\left(\frac{\partial \varphi_1}{\partial x_1} + \vartheta\frac{\partial \varphi_2}{\partial x_2}\right) + \left(\frac{\partial u_0}{\partial x_1} + \vartheta\frac{\partial v_0}{\partial x_2}\right) - x_3\frac{\partial^2 w}{\partial x_1^2} + \vartheta\frac{\partial^2 w}{\partial x_2^2}\right] \qquad (6a)$$

$$\sigma_{22} = \frac{E(x_3)}{1-\vartheta^2}(\varepsilon_{22} + \vartheta\varepsilon_{11}) = \frac{E(x_3)}{1-\vartheta^2}\left[f(x_3)\left(\frac{\partial \varphi_2}{\partial x_2} + \vartheta\frac{\partial \varphi_1}{\partial x_1}\right) + \left(\frac{\partial v_0}{\partial x_2} + \vartheta\frac{\partial u_0}{\partial x_1}\right) - x_3\frac{\partial^2 w}{\partial x_2^2} + \vartheta\frac{\partial^2 w}{\partial x_1^2}\right] \qquad (6b)$$

$$\tau_{12} = G\gamma_{12} = \frac{E(x_3)}{2(1+\vartheta)}\left(\frac{\partial u_0}{\partial x_2} + \frac{\partial v_0}{\partial x_1} - 2x_3\frac{\partial^2 w}{\partial x_1 \partial x_2} + f(x_3)\left(\frac{\partial \varphi_1}{\partial x_2} + \frac{\partial \varphi_2}{\partial x_1}\right)\right) \qquad (6c)$$

$$\tau_{13} = G\gamma_{13} = \frac{E(x_3)}{2(1+\vartheta)}\left(\frac{df(x_3)}{dx_3}\varphi_1\right) \qquad (6d)$$

$$\tau_{23} = G\gamma_{23} = \frac{E(x_3)}{2(1+\vartheta)}\left(\frac{df(x_3)}{dx_3}\varphi_2\right) \qquad (6f)$$

where $E(x_3)$ is the Young's modulus and $G(x_3) = E(x_3)/2(1+\vartheta)$ is the Shear modulus of the plate. The Hamilton's principle was employed to extract equation of motion. The Hamilton's principle can be defined as follows [13]:

$$\int_0^T (\delta U + \delta W - \delta T)dt = 0 \qquad (7)$$

where δ is the variation operator, U is the strain energy, W is the work done by external forces and T is the kinetic energy. U, T, and W in the Eq. (7) can be defined as below:

$$U = \frac{1}{2}\int_v (\varepsilon_{11}\sigma_{11} + \varepsilon_{22}\sigma_{22} + 2\varepsilon_{12}\sigma_{12} + 2\varepsilon_{13}\sigma_{13}$$

$$+ 2\varepsilon_{23}\sigma_{23}) \qquad (8)$$

$$T = \frac{1}{2}\int_v \rho(x_3)(\dot{u}^2 + \dot{v}^2 + \dot{w}^2)dv \qquad (9)$$

$$W = \frac{1}{2}\int_0^a \int_a^b \left[N_1\left(\frac{\partial w}{\partial x_1}\right)^2 + N_2\left(\frac{\partial w}{\partial x_2}\right)^2\right]dydx \qquad (10)$$

where dot-top index contract indicates the differentiation with respect to the time variable and N_1 and N_2 are the in-plane loads in the x_1 and x_2 directions respectively. Exertion of variation operator on Eq. (7) should be as follows:

$$\delta\left(\frac{\partial i}{\partial j}\right) = \frac{\partial}{\partial j}\delta(i), \qquad i = \varphi_1, \varphi_2 \quad j = x_1, x_2 \quad (11)$$

$$\delta\left(\frac{\partial^2 i}{\partial j\partial k}\right) = \frac{\partial^2}{\partial j\partial k}\delta(i) \qquad i = w, \begin{cases} j = x_1, x_2 \\ k = x_1, x_2 \end{cases} \quad (12)$$

$$\delta\left(\frac{\partial i}{\partial t}\right)^2 = 2\left(\frac{\partial i}{\partial j}\right)\frac{\partial}{\partial j}\delta(i), \quad i = u, v, w \qquad (13)$$

Finally, the nonlocal governing differential equations of motion of the rectangular nanoplates in terms of the stress resultants were derived by Hamilton's principle (using Eq. (7)), which can be defined as Eqs. (14a) - (14e).

$$\frac{\partial N_{11}}{\partial x_1} + \frac{\partial N_{12}}{\partial x_2} = I_0\left(\frac{\partial^2 u_0}{\partial t^2}\right) - I_1\left(\frac{\partial^3 w}{\partial x_1\partial t^2}\right) + I_3\left(\frac{\partial^2 \varphi_1}{\partial t^2}\right) \qquad (14a)$$

$$\frac{\partial N_{22}}{\partial x_2} + \frac{\partial N_{12}}{\partial x_1} = I_0\left(\frac{\partial^2 v_0}{\partial t^2}\right) - I_1\left(\frac{\partial^3 w}{\partial x_2\partial t^2}\right) + I_3\left(\frac{\partial^2 \varphi_2}{\partial t^2}\right) \qquad (14b)$$

$$\frac{\partial^2 M_{11}}{\partial x_1^2} + 2\frac{\partial^2 M_{12}}{\partial x_2\partial x_2} + \frac{\partial^2 M_{22}}{\partial x_2^2} = I_0\left(\frac{\partial^2 w}{\partial t^2}\right) + I_1\left(\frac{\partial^3 u_0}{\partial x_1\partial t^2} + \frac{\partial^3 v_0}{\partial x_2}\partial t^2\right) - I_2\left(\frac{\partial^4 w}{\partial x_1^2\partial t^2} + \frac{\partial^4 w}{\partial x_2^2\partial t^2}\right)$$

$$+ I_4\left(\frac{\partial^3 \varphi_1}{\partial x_1\partial t^2} + \frac{\partial^3 \varphi_2}{\partial x_2\partial t^2}\right) + N_1\frac{\partial^2 w}{\partial x_1^2} + N_2\frac{\partial^2 w}{\partial x_2^2} \qquad (14c)$$

$$\frac{\partial R_{11}}{\partial x_2} + \frac{\partial R_{12}}{\partial x_1} - Q_1 = I_3\left(\frac{\partial^2 u_0}{\partial t^2}\right) - I_4\left(\frac{\partial^3 w}{\partial x_1\partial t^2}\right) + I_5\left(\frac{\partial^2 \phi}{\partial t^2}\right) \qquad (14d)$$

$$\frac{\partial R_{22}}{\partial x_2} + \frac{\partial R_{12}}{\partial x_1} - Q_2 = I_3\left(\frac{\partial^2 v_0}{\partial t^2}\right) - I_4\left(\frac{\partial^3 w}{\partial x_2\partial t^2}\right) + I_5\left(\frac{\partial^2 \varphi_2}{\partial t^2}\right) \qquad (14e)$$

The following sets of boundary conditions at the edges of the plate were obtained as a result of the application of the Hamiltons principle:

Either $R_{11} = 0$ or φ_1 prescribed at $x_1 = 0, a$

and either $R_{22} = 0$ or φ_2 prescribed at $x_2 = 0, b$ (15a)

Either $R_{12} = 0$ or φ_2 prescribed at $x_1 = 0, a$

and either $R_{12} = 0$ or φ_1 prescribed at $x_2 = 0, b$ (15b)

Either $M_{11} = 0$ or $\frac{\partial x_3}{\partial x_1}$ prescribed at $x_1 = 0, a$

and either $M_{22} = 0$ or $\frac{\partial x_3}{\partial x_2}$ prescribed at $x_2 = 0, b$ (15c)

Either $\frac{\partial M_1}{\partial x_1} + 2\frac{\partial M_{12}}{\partial x_2} = 0$ or x_3 prescribed at $x_1 = 0, a$

and either $\frac{\partial M_2}{\partial x_2} + 2\frac{\partial M_{12}}{\partial x_1} = 0$ prescribed at $x_2 = 0, b$

(15d)

Either $N_{11} = 0$ at $x_1 = 0, a$ and either

$N_{22} = 0$ prescribed at $x_2 = 0, b$ (15e)

where

$$(I_0, I_1, I_2, I_3, I_4, I_5) =$$

$$\int_{-\frac{h}{2}}^{\frac{h}{2}} \rho(x_3, T)(1, x_3, x_3^2, f(x_3), x_3 f(x_3))dx_3 \qquad (16a)$$

$$(R_{11}, R_{22}, R_{12}) = \int_{-\frac{h}{2}}^{\frac{h}{2}} (\sigma_{11}, \sigma_{22}, \sigma_{12}) f(x_3) dx_3 \quad (16b)$$

$$(Q_1, Q_2) = \int_{-\frac{h}{2}}^{\frac{h}{2}} (\sigma_{13}, \sigma_{23}) \left(\frac{df(x_3)}{dx_3} \right) dx_3 \quad (16c)$$

$$(N_{11}, N_{22}, N_{12}) = \int_{-\frac{h}{2}}^{\frac{h}{2}} (\sigma_{11}, \sigma_{22}, \sigma_{12}) dx_3 \quad (16d)$$

$$(M_{11}, M_{22}, M_{12}) = \int_{-\frac{h}{2}}^{\frac{h}{2}} (\sigma_{11}, \sigma_{22}, \sigma_{12}) x_3 dx_3 \quad (16e)$$

where I is the intertia, N, R and Q are the stress resultants and M is the moment which is acting on the body. It can be inferred that in Eqs. (16a)-(16e) the functions of displacements are coupled. The permissible displacement and rotation functions that can satisfy the simply supported boundary conditions at all edges of the plate are trigonometric series. According to the Navier solution, the explanation of the displacements and rotations are [11]:

$$u_0 = \sum_{m=1}^{\infty} \sum_{n=1}^{\infty} u_{mn} \cos(\gamma x) \sin(\beta y) \sin(\lambda_{mn} t) \quad (17a)$$

$$v_0 = \sum_{m=1}^{\infty} \sum_{n=1}^{\infty} v_{mn} \sin(\gamma x) \cos(\beta y) \sin(\lambda_{mn} t) \quad (17b)$$

$$w = \sum_{m=1}^{\infty} \sum_{n=1}^{\infty} W_{mn} \sin(\gamma x) \cos(\beta y) \sin(\lambda_{mn} t) \quad (17c)$$

$$\varphi_1 = \sum_{m=1}^{\infty} \sum_{n=1}^{\infty} \phi_{mn} \sin(\gamma x) \cos(\beta y) \sin(\lambda_{mn} t) \quad (17d)$$

$$\varphi_2 = \sum_{m=1}^{\infty} \sum_{n=1}^{\infty} \psi_{mn} \sin(\gamma x) \cos(\beta y) \sin(\lambda_{mn} t) \quad (17e)$$

where $(u_{mn}, v_{mn}, W_{mn}, \phi_{mn}, \psi_{mn})$ are unknown constant coefficients and λ_{mn} is the natural frequency of the plate. Substituting Eqs. (17a)-(17e) into (14a)-(14e) and setting λ_{mn} as zero, the formulation of buckling problem is yielded as the following form:

$$([K] - N_{cr}[K_g])[\Delta] = 0 \quad (18)$$

Where $[K]$ collects all stiffness terms, $[K_g]$ collects all terms related to the in-plane forces and $[\Delta]$ is the vector of unknown coefficients. For each value of m and n, the smallest value of N_{cr} is the critical buckling load of the plate.

3. Results and Discussion

In order to validate the present formulation, the critical buckling load of FG (Al/Al$_2$O$_3$) rectangular plate obtained by the present method were compared with those of Şimşek Reddy (2013) as listed in Table 2 and Table 3. In Tables 2 and 3, the non-dimensional critical buckling load, $N_{cr} = \frac{N_{cr} a^2}{D}$ of a simply supported FG rectangualr plate are reported for different plate's aspect ratios including $\frac{a}{b} = 0.5, 1.0, 1.5$ and 2.0, and plate's length to thickness ratios $\frac{a}{h} = 5, 10$ and 20, and power low indexes of the FG material $g = 0, 1, 2$ and 10. In Tables 2 and 3 calculations are illustrated for the FG rectangular plate which subjected to uniaxial compression load along the x_1-axis ($\beta_1 = -1, \beta_2 = 0$) and biiaxial compression load ($\beta_1 = -1, \beta_2 = -1$) respectively. From the results presented in Tables 2 and 3, it can be seen that there is a good agreement between the present results and those of Şimşek Reddy (2013).

Table 2
Comparison of non-dimensional critical buckling load ($\bar{N}_{cr}$) of FG plate subjected to uniaxial compression load along the x_1-axis ($\beta_1 = -1, \beta_1 = 0$).

a/b	h/a	Source	Power low index			
			0	1	1	10
		Present	6.7259	3.1488	2.6457	1.9209
	5	Şimşek Reddy (2013)	6.7203	3.4164	2.6451	1.9213
		Present	7.4069	3.7118	2.8898	2.1894
0.5	10	Şimşek Reddy (2013)	7.4050	3.7100	2.8800	2.1800
		Present	7.5997	3.7932	2.9582	2.2689
	10	Şimşek Reddy (2013)	7.5990	3.7900	2.9500	2.2600
		Present	16.1425	8.2340	6.3459	4.4801
	5	Şimşek Reddy (2013)	16.0200	8.2200	6.3400	4.4800
		Present	18.5847	9.3418	7.2636	5.4521
1.0	10	Şimşek Reddy (2013)	18.5700	9.3300	7.2600	5.4500
		Present	19.3544	9.6682	7.5372	5.7666
	10	Şimşek Reddy (2013)	19.3500	9.6600	7.5300	5.7600

Table 3

Comparison of non-dimensionalcriticalbucklingload ($\bar{N}_{cr}$) of FG plate subjected to biaxial compression loads ($\beta_1 = -1, \beta_2 = -1$).

a/b	h/a	Source	Power low index			
			0	1	1	10
		Present	5.3807	2.7350	2.1166	1.5367
	5	Şimşek Reddy (2013)	5.3760	2.7330	2.1160	1.5370
		Present	5.9255	2.9694	2.3118	1.7515
0.5	10	Şimşek Reddy (2013)	5.9260	2.9690	2.3120	1.7520
		Present	6.0797	3.0346	2.3665	1.8151
	10	Şimşek Reddy (2013)	6.0790	3.0340	2.3670	1.8150
		Present	8.0212	4.1170	3.1729	2.2400
	5	Şimşek Reddy (2013)	8.0110	4.1120	3.1720	2.2400
		Present	9.2924	4.6709	3.6318	2.7260
1.0	10	Şimşek Reddy (2013)	9.2890	4.6700	3.6320	2.7260
		Present	9.6772	4.8341	3.7686	2.8833
	10	Şimşek Reddy (2013)	9.6760	4.8340	3.7690	2.8830
		Present	10.6945	6.9969	5.4085	3.8967
	5	Şimşek Reddy (2013)	11.6820	6.0800	4.6640	3.1720
		Present	14.1659	7.6862	5.9820	4.5211
1.5	10	Şimşek Reddy (2013)	14.6080	7.3790	5.7280	4.2380
		Present	15.4289	7.8809	6.1455	4.7105
	10	Şimşek Reddy (2013)	15.5890	7.7980	6.0760	4.6300
		Present	15.7757	8.3338	6.3456	4.1421
	5	Şimşek Reddy (2013)	15.7240	8.3090	6.3350	4.1380
		Present	21.5230	10.9402	8.4662	6.1467
2.0	10	Şimşek Reddy (2013)	21.5050	10.9320	8.4640	6.1480
		Present	23.7020	11.8776	9.2473	7.0060
	10	Şimşek Reddy (2013)	23.6970	11.8750	9.2470	7.0070

In Fig. 2, the influence of the length to thickness ratios, (a/h), on the non-dimensional critical buckling load, $\bar{N}_{cr} = \dfrac{N_{cr}a^2}{D}$, is illustrated for a functionally graded (Al/Al$_2$O$_3$) rectangular plate with simply supported boundary conditions while gradient index, g, varies from 0 to 10. From the results presented in Tables 2 and 3 and Fig. 2, it can be observed that the non-dimensional critical buckling load of the FG rectangular plate increases monotonically, as the length to thickness ratio increases. This isn't a surprising result since we know higher values of length to thickness ratios reduce the stiffness of the structure more effectively than its inertia, thus lower value of the critical buckling load and higher value of the non-dimensional critical buckling load, $\bar{N}_{cr} = \dfrac{N_{cr}a^2}{D}$, should be expected.

Variation of non-dimensional critical buckling load, $\bar{N}_{cr} = \dfrac{N_{cr}a^2}{D}$, of a functionally graded (Al/Al$_2$O$_3$) rectangular plate versus plate's aspect ratio are illustrated in Fig. 3 for simply supported boundary conditions while the aspect ratios of the plates vary from 0.5 to 3. From the results presented in Fig. 3, it can be observed that the non-dimensional critical buckling load are considerably increased by increasing the aspect ratio of plate.

From Figs. 2 and 3 it can be observed that by increasing the value of the power law index leads to re-duction of the amplitude of the critical buckling load. This is due to the fact that higher values of power law index correspond to high portion of metal in comparison with the ceramic part. In other words, increase in the power-law index results in reduction of elasticity modulus and bending stiffnes implying that the plate becomes flexible. Therefore, it leads to reduction of the critical buckling load.
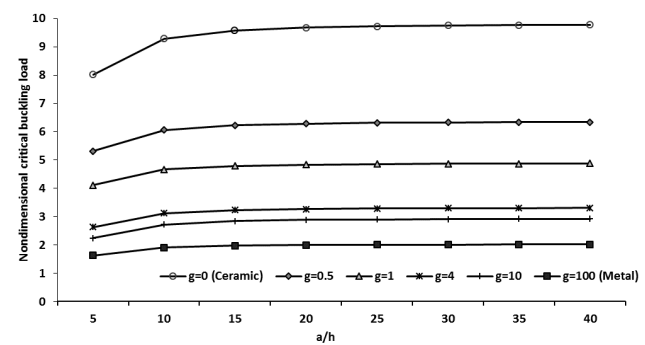

Fig. 2. Effect of length to thickness ratios (a/h) on non-dimensionalcritical buckling load under biaxial compression load.

4. Conclusions

A Navier method was applied to analysis buckling of functionally graded rectangular plates. The formulations were based on exponential shear deformation the-

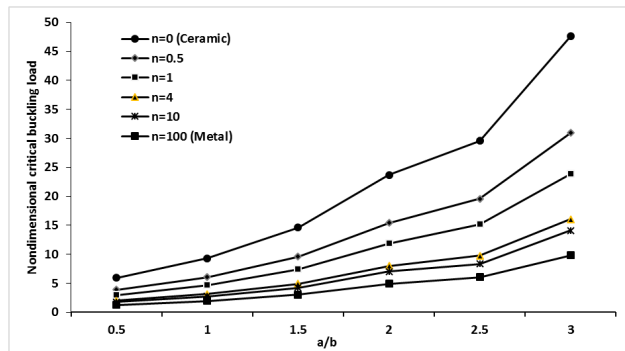ory and Hamilton's principle isused to derive the equations of motion and associated boundary conditions.

Fig. 3. Effect of aspect ratio (a/b) on non-dimensionalcritical buckling load under biaxial compression for an FG plate and various material variation parameters(n).

Comparison cases by those reported in the literature for simply supported rectangular FG plates demonstrate high stability and accuracy of the present solution. Presented results herein show the effects of variations of thickness to length ratio, power law indexes, and aspect ratio on the critical values of an FG plate. It was shown that increase in the power law index causes the non-dimensional critical buckling to decrease, Also, The increase of aspect ratio increases the critical buckling load, and increase in the length to thickness causes increase in the critical buckling load. All analytical results presented here can provide other research groups with a reliable source to inspect their analytical and numerical solutions.

References

[1] E. Reissner, The effect of transverse shear deformation on the bending of elastic plates, J. Appl. Mech-T ASME., 12 (1945) 69-77.

[2] R.D. Mindlin, Influence of rotatory inertia and shear on flexural motions of isotropic, elastic plates, J. Appl. Mech-T ASME., 18 (1951) 31-38.

[3] B. Mokhtar, T. Abedlouahed, A. Abbas, M. Abdelkader, Buckling analysis of functionally graded plates with simply supported edges, Leonardo J. Sci., 8 (2013) 21-32.

[4] M. Şimşek, J.N. Reddy, Bending and vibration of functionally graded microbeams using a new higher order beam theory and the modified couple stress theory, Int. J. Eng. Sci., 64 (2013) 37-53.

[5] H. Matsunaga, Free vibration and stability of functionally graded plates according to a 2-D higher-order deformation theory, Compos. Struct., 82 (2008) 499-512.

[6] S. Yahia, H.A. Atmane, M.S.A. Houari, A. Tounsi, Wave propagation in functionally graded plates with porosities using various higher-order shear deformation plate theories, Struct. Eng. Mech., 53(6) (2015) 1143-1165.

[7] P. Malekzadeh, A.A. Beni, Free vibration of functionally graded arbitrary straight-sided quadrilateral plates in thermal environment, Compos. Struct., 92 (2010) 2758-2767.

[8] V. Ungbhakorn, N. Wattanasakulpong, Thermoelastic vibration analysis of third-order shear deformable functionally graded plates with distributed patch mass under thermal environment, Appl. Acousf., 74 (2013) 1045-1059.

[9] J. Reddy, Microstructure-dependent couple stress theories of functionally graded beams, J. Mech. Phys. Solid., 59(11) (2011) 2382-2399.

[10] A.S. Sayyad, Y.M. Ghugal, Bending and free vibration analysis of thick isotropic plates by using exponential shear deformation theory, Appl, Comput, Mech., 6(1) (2012) 65-82.

[11] K. Khorshidi, Effect of hydrostatic pressure on vibrating rectangular platescoupled with fluid, Sci. Iran: Trans A: Civ. Eng., 17(6) (2010) 41529.

[12] N.R. Senthilnathan, K.H. Lim, K.H. Lee, S.T. Chow, Buckling of shear deformable plates. AIAA J., 25(9) (1987) 1268-71.

[13] K. Khorshidi, M. Khodadadi, Precision closed-form solution for out-of-plane vibration of rectangular plates via trigonometric shear deformation theory, Compos. Struct., 3(1) (2016) 31-43.

[14] K. Khorshidi, M. Pagoli, Analytical solution for sound radiation of vibrating circular plates coupled with piezo-electric layers, Compos. Struct., 3(2) (2016) 89-98.

[15] H.T. Thai, D.H. Choi, Size-dependent functionally graded Kirchhoff and Mindlin plate models based on a modified couple stress theory, Compos. Struct., 95 (2013) 142-153.

[16] K. Khorshidi, S. Farhadi, Free vibration analysis of a laminated composite rectangular plate in contact with a bounded fluid, Compos. Struct., 104 (2013) 176-186.